Chapter 12

Ultrafast Optical Spectroscopy of Photosystem I

Sergei Savikhin*
Department of Physics, Purdue University, West Lafayette, IN 47907, USA

Summary

This review discusses energy and electron transfer in Photosystem I (PS I) complexes by means of ultrafast time-resolved optical techniques. In particular, this article addresses directly observable initial (sub)picosecond electronic excitation equilibration among different antenna chlorophyll forms and energy trapping by the charge separation process followed by picosecond electron transfer to the secondary electron acceptor A_1. There is still no general agreement on the energy trapping classification in PS I; the validity of diffusion-limited, trap-limited, and mixed-energy trapping models is tested against the available experimental data. Ultrafast experiments on branch-specific complementary mutants of the reaction center open the unique possibility of differentiating between the two highly symmetrical branches of the reaction center, revealing the directionality of electron transfer in PS I. Finally, the most recent optical data questions the conventional sequence of electron transfer steps, and suggests the intriguing possibility that one additional intermediate radical pair may exist that was not previously observed.

I. Introduction

A. General Remarks

Photosystem I (PS I) is a chlorophyll–protein complex that uses light energy to reduce ferredoxin in cyanobacteria and plants (Brettel, 1997). The primary events triggered by light absorption in the core antenna–reaction center of PS I complexes have been intensively studied by ultrafast spectroscopy since the mid-1980s (van Grondelle et al., 1994). Recent determination and subsequent refinements of the X-ray crystal structure of the PS I core antenna–reaction center (RC) complex from the cyanobacterium *Synechococcus elongatus* (Krauß et al., 1993, 1996; Klukas et al., 1999; Jordan et al., 2001) and from a higher plant

*Author for correspondence, email: sergei@physics.purdue.edu

John H. Golbeck (ed), The Light-Driven Plastocyanin, 155–175.

Author: The spelling "Krauss" has been changed to "Krauß" in order to match with the references list.

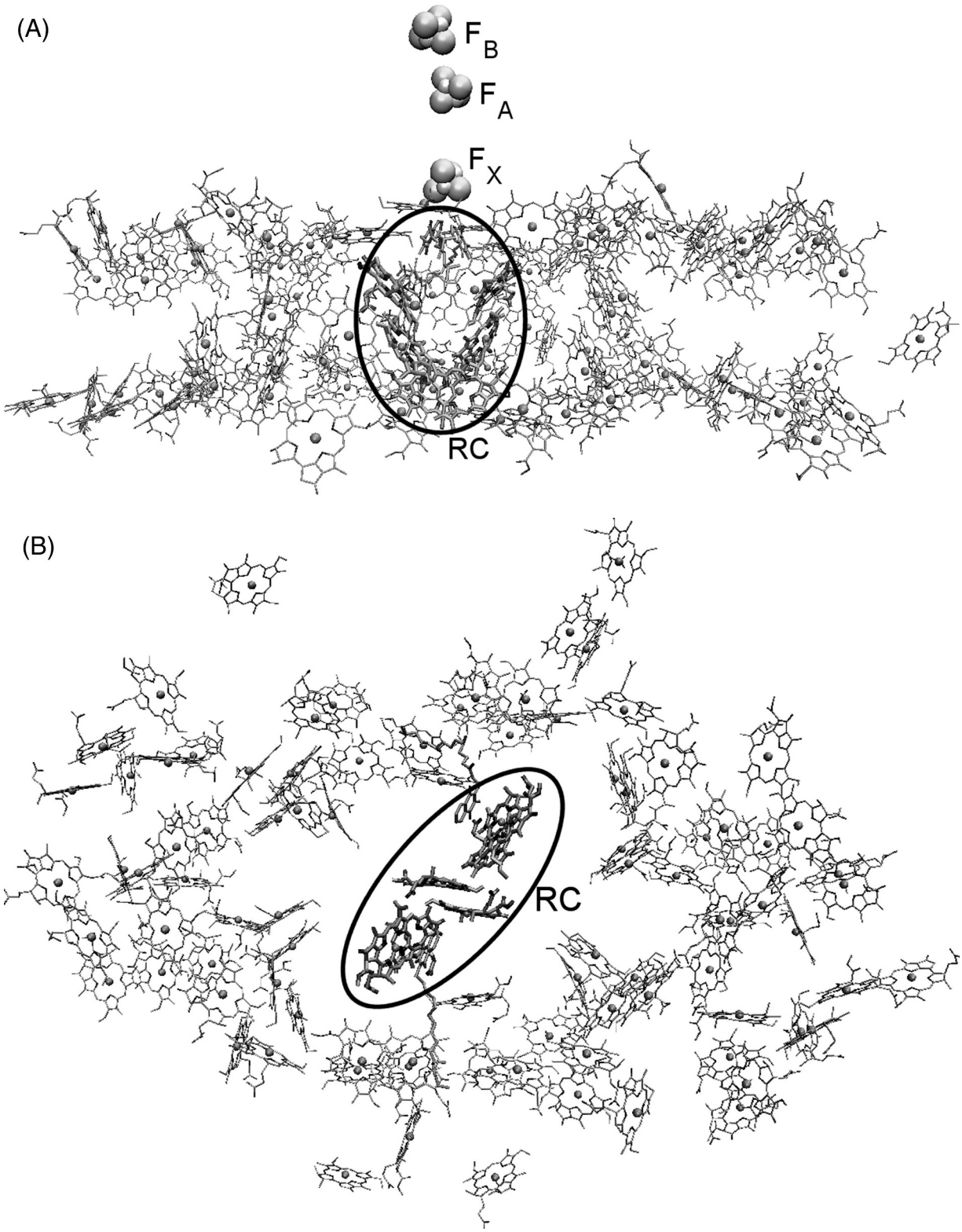

Fig. 1. Arrangement of the pigments and iron–sulfur cofactors within the PS I core complexes from *Synechococcus elongatus*. (A) Side view. (B) Top view (Jordan et al., 2001).

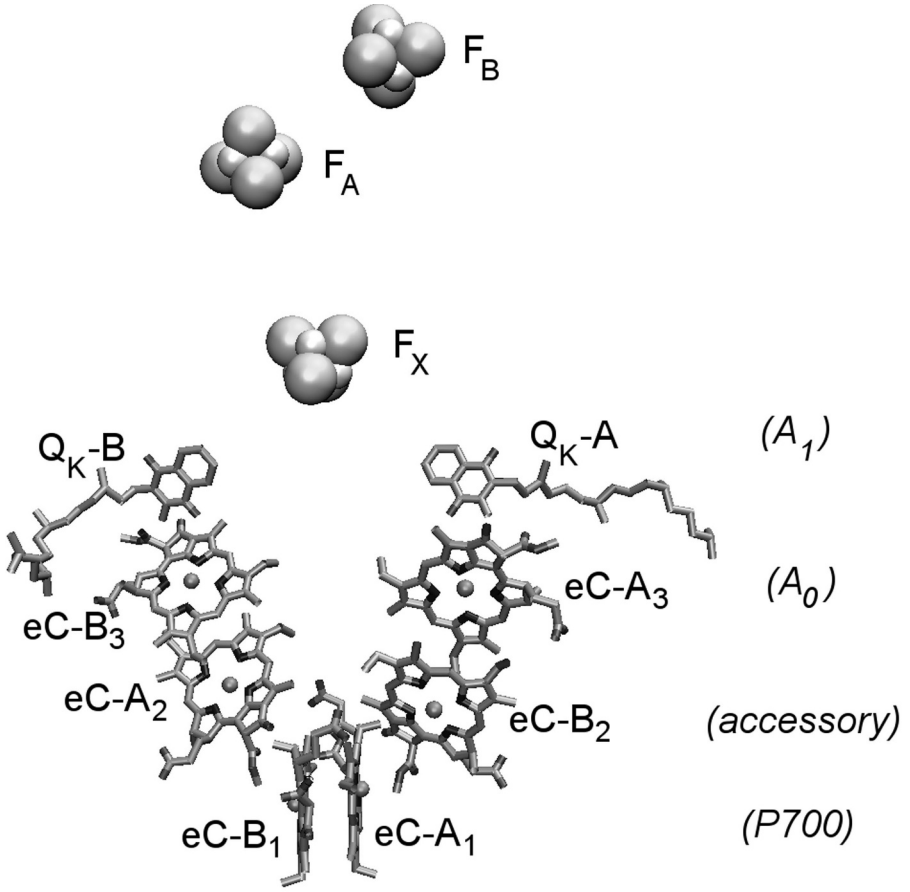

Fig. 2. Arrangement of electron transfer cofactors in PS I (Jordan et al., 2001).

(Ben-Shem et al., 2003) has prompted a resurgence of interest in primary processes in PS I and made structure-based modeling of energy and electron transfers possible in this photosynthetic complex. These simulations, while leading to a deeper molecular understanding of the structure–function relationships in PS I, rely heavily on the available experimental data on the dynamics of the modeled processes. Energy transfer, charge separation, and primary electron transfer (ET) steps in PS I all occur competitively during the first 20–50 psec after absorption of a photon and can be best monitored by means of ultrafast optical spectroscopy.

In this chapter, we summarize investigations of the ultrafast dynamics of electronic energy transfer from the PS I antenna to the PS I RC followed by rapid charge separation and the first electron transfer step.

Abbreviations: Chl – chlorophyll; DAS – decay-associated spectrum; ESA – excited state absorption; ET – electron transfer; PB – photobleaching; PS – photosystem; RC – reaction center; SE – stimulated emission.

B. The Structure of the Photosystem I Complex

According to the latest X-ray data, the cyanobacterial PS I core complex contains one chlorophyll (Chl) *a*′ and 95 Chl *a* pigments, which are coordinated by several protein subunits (Jordan et al., 2001; see Fromme and Grotjohann, this volume, Chapter 6). Most of the pigments function as light-harvesting antenna, capturing light excitation and transferring it to the RC located in the middle of the PS I complex. The antenna pigments are arranged in a quasielliptical manner (Fig. 1A) around the reaction center with the only hint of pseudo-C_2 symmetry. The side view (Fig. 1B) reveals that 79 of all identified Chls form two distinct layers near and parallel to the stromal and lumenal membrane surfaces, respectively. The RC is located in the middle of the complex and is comprised of six Chl cofactors (Fig. 2):

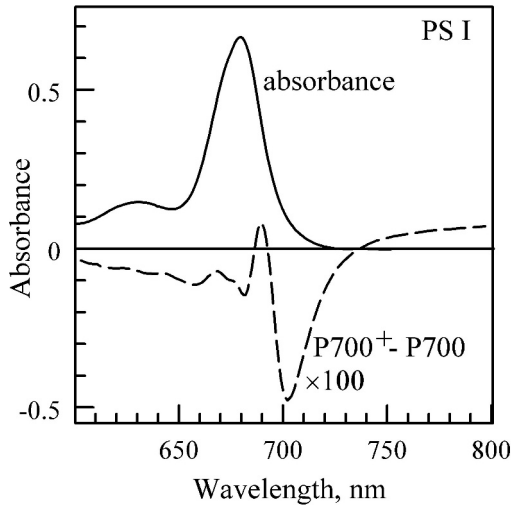

Fig. 3. Steady-state absorption (solid line) and ($P700^+ - P700$) absorption difference spectrum (dashed) of PS I core complexes from *Synechocystis* sp. at room temperature.

the primary electron donor P700 (a heterodimer of Chl a' and a denoted as eC-A_1 and eC-B_1, respectively), two accessory Chls (eC-B_2 and eC-A_2), and two chlorophylls denoted as eC-A_3 and eC-B_3, of which one or both are believed to serve as primary electron acceptor A_0. According to the conventional model, in the PS I RC, primary charge separation leads to the reduction of A_0, creating the radical ion-pair $P700^+A_0^-$. The unpaired electron migrates first to the phylloquinone secondary acceptor A_1 (Q_K-A and/or Q_K-B), then to the [4Fe–4S] center F_X, and finally to the terminal iron–sulfur centers F_A and F_B before being transferred to ferredoxin (Brettel, 1997; Brettel and Leibl, 2001).

The mean distance from any of the antenna pigments to its nearest neighbor in the PS I core complex is 9.9 Å, and the average distance to the second- and third-nearest pigments are 12.2 and 14.3 Å, respectively. Such close proximity of antenna pigments to each other ensures rapid and efficient excitation energy equilibration between antenna pigments and excitation transfer to the RC. A simple estimate based on the Förster energy transfer theory (Struve, 1995) predicts that the single-energy transfer step between the neighboring pigments in PS I occurs in 100–200 fsec. The overall lifetime of electronic excitation in the antenna has been shown to be ~20–60 psec depending on the species (Holzwarth et al., 1998; Karapetyan et al., 1999; Gobets and van Grondelle, 2001; Melkozernov, 2001), which implies that ~100 single-energy transfer steps occur before the electronic excitation reaches the RC and gets trapped, forming the $P700^+A_0^-$ charge separated state. Experimental observation of each individual energy transfer step in such a complex system is impossible; instead, only a small number of average kinetic processes can be distinguished.

Optical transition energies of Chl *a* pigments in PS I strongly overlap—the Q_y absorption band measured for PS I complexes is ~30 nm wide (Fig. 3), while an individual Chl *a* molecule yields an absorption band which is only three times narrower at room temperature. Such spectral congestion, combined with uncertainties in optical transition energies, further complicates detailed analysis of experimental data and modeling of the energy transfer process in PS I. The exact transition energies have only been measured for the special pair P700 and the primary electron acceptor A_0. The former is characterized by a broad (~30 nm fwhm) absorption band centered at ~700 nm, and the latter has been measured to absorb at ~686 nm and has an absorption bandwidth of ~10 nm (Hastings et al., 1994b; Savikhin et al., 2001). Spectral positions of other Chls have recently been derived using structure-based theoretical simulations (Byrdin et al., 2002; Damjanovic et al., 2002), though these predictions could not be experimentally verified. One of the striking features of all PS I complexes is the presence of a relatively small number of Chls that absorb at energies lower than that of the primary electron donor P700 (Shubin et al., 1991; Wittmershaus et al., 1992; van der Lee et al., 1993; Gobets et al., 1994; Pålsson et al., 1996, 1998; Melkozernov et al., 2000; see Karapetyan et al., this volume, Chapter 13). Although the number of these low energy Chls is small, they have a pronounced effect on the overall energy transfer and trapping process since an energy transfer from these "red" pigments to the primary electron donor P700 occurs uphill and is therefore relatively slow.

The primary charge separation in PS I is followed by a rapid electron transfer step from A_0^- to the secondary electron acceptor A_1^-. The intrinsic rate of this electron transfer step (~0.03–0.1 $psec^{-1}$)is comparable to the antenna lifetime and cannot be directly observed in experiments. The formation of $P700^+A_0A_1^-$ concludes the sequence of events, which can be monitored by ultrafast spectroscopy techniques. The subsequent electron transfer steps occur on a time scale of >10 nsec and will be not addressed in this chapter.

II. Ultrafast Optical Spectroscopy Techniques

During past decades, energy and electron transfer in PS I have been studied by several ultrafast

spectroscopy techniques: pump–probe absorption spectroscopy (Holzwarth et al., 1993; Kumazaki et al., 1994a; Hastings et al., 1994b; Hastings et al., 1995b; Melkozernov et al., 2000; Savikhin et al., 2000; Kumazaki et al., 2001; Savikhin et al., 2001; Müller et al., 2003), single-photon counting (Werst et al., 1992; Holzwarth et al., 1993; Turconi et al., 1993; Pålsson et al., 1995), fluorescence upconversion (Du et al., 1993; Kennis et al., 2001), and synchroscan streak camera techniques (Gobets et al., 2001).

In a typical pump–probe absorption experiment, a short laser pulse (pump pulse) is used to excite one of the pigments (typically Chl) within the PS I complex. As the pigment is promoted into an excited state the absorption spectrum of the whole PS I complex changes, reflecting the optical properties of the excited molecule. The resulting difference between the absorption spectrum before excitation and that after excitation (ΔA) is then probed as a function of wavelength and time by a second light pulse (probe pulse). When the excitation energy is transferred between spectrally distinct molecules or is trapped, the dynamics of this process is reflected in the dynamics of the ΔA signal. There are three major contributions to the absorption difference signal when a molecule is excited: photobleaching (PB) of the original absorption spectrum of the excited molecule, excited state absorption (ESA) that arises from the transitions in the excited molecule to higher excited states, and stimulated emission (SE) due to the stimulated transition from the excited state to the ground state of the excited molecule. These three components of the ΔA signal are superimposed on each other and, in general, cannot be measured independently in a pump–probe experiment. The time resolution of a modern ultrafast pump–probe spectrometer is determined only by the duration of the laser pulse and can be better than 100 fsec—a resolution sufficient to resolve a single-energy transfer step in PS I. The sensitivity of the ΔA signal to both the ground and excited state populations allows not only detection of excitation energy transfer dynamics, but also electron transfer kinetics which involve optically visible cofactors such as P700, A_0, and phylloquinone A_1 (the latter has a distinct absorption band at ~380 nm). However, the primary electron transfer steps occur within the same time range as excitation energy transfer processes, and separating the signals due to the different processes is not straightforward.

Single-photon counting, fluorescence upconversion, and synchroscan streak camera techniques all detect transient fluorescence and therefore can monitor only the dynamics of optically active excited states. The main difference between these methods lies in their light sensitivity and time resolution. Single-photon counting and the synchroscan streak camera can both work with very low fluorescence intensities, but their time resolution is limited to ~10 and ~1 psec, respectively. In contrast, fluorescence upconversion techniques can deliver time resolution better than 100 fsec, but have poor light sensitivity due to the non-linear process utilized in the detection scheme.

A single PS I complex contains a coupled network of 96 Chls. Under natural sunlight intensities, a single Chl molecule gets excited less than 10 times per second, and there is never more than one excitation at a time in a single PS I complex. Creating two or more excitations in a PS I complex in experiments utilizing short laser pulses may lead to an effect called singlet–singlet annihilation (van Grondelle, 1985; Valkunas et al., 1995b; Gobets and van Grondelle, 2001), which can seriously distort experimental data. Due to efficient energy transfer, two excitations can collide at a single chlorophyll, promoting it to its second excited state. The following rapid internal conversion to the lowest excited state effectively quenches one of the excitations, adding a nonphysiological component to the measured signal. Alternatively, even if one of the excitations is trapped in a normal way and initiates electron transfer, the oxidation of P700–$P700^+$ effectively closes the normal physiological trapping path for the second excitation, resulting in similar artifacts in the measured transient signal. It was shown, for example, that under intense excitation conditions when 4–8 excitations were created per a single PS I complex, annihilation shortened the natural excitation lifetime in the antenna from 20–30 to 4–5 psec (Hastings et al., 1994b). Due to the probabilistic nature of the excitation process, it is not sufficient to simply match the number of absorbed photons to the number of complexes in the same volume. One can easily show that the ratio of excitations in multiple excited complexes to the total number of excitations is given by $n_{\mathrm{mult}}/n_{\mathrm{tot}} = 1 - (1-p)^{N-1}$, where $N = 96$ is the number of molecules in a single complex, and p is the absolute fraction of excited Chl molecules. In the case of $p = 1/96$ (i.e., one excitation is created per single complex on average), the fraction of multiple excitations contributing to annihilation artifacts is 63%. To keep this fraction below 10%, each laser shot should excite not more than one out of ~10 PS I complexes. In practice, this implies that excitation pulse energies must be of the order of a *nJ* and the detection system should be capable of detecting absorption changes ΔA smaller than 10^{-3}.

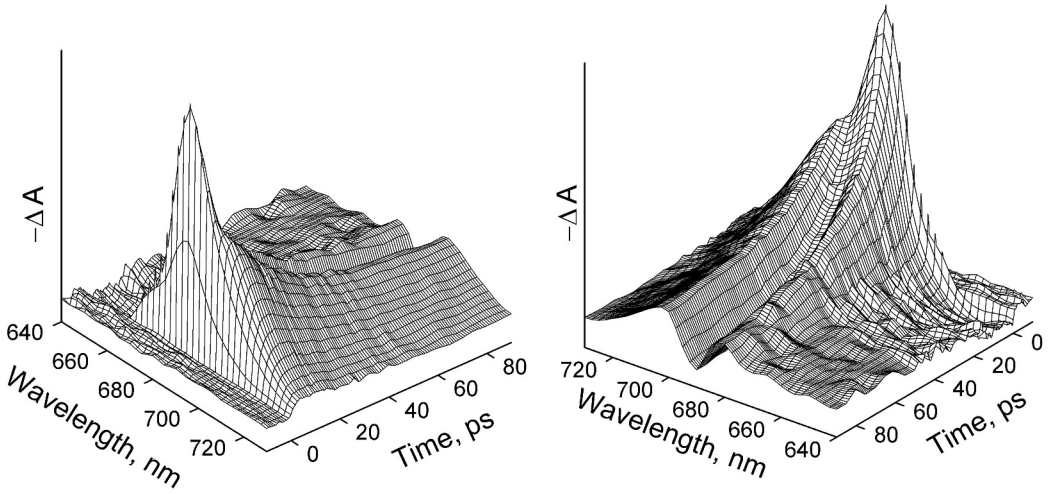

Fig. 4. Two different perspectives of ΔA versus time and wavelength surfaces for PS I core complexes from *Synechocystis* sp. measured at room temperature upon excitation at 660 nm.

Excitation trapping in the PS I complex switches the special pair from the neutral P700 state to the oxidized $P700^+$ state, often referred to as the open and closed states of the RC (or PS I), respectively. When the RC is in a closed state, the normal charge separation function of PS I is disrupted and electronic excitation in the PS I antenna is quenched by a nonphysiological process. To avoid this, sufficient time must be allowed between the consequent excitation pulses to ensure full recovery of the RC to its open state, or, alternatively, a sample should be physically circulated through the laser beam rapidly enough to ensure that every light pulse excites fresh complexes with open RCs. It has been shown that recombination between $P700^+$ and the reduced terminal acceptor $[F_A/F_B]^-$ occurs within 45 msec (Hiyama and Ke, 1971). However, after each excitation, a fraction of electrons on the terminal electron acceptors are scavenged from the PS I complexes (Diaz-Quintana et al., 1998) before recombination can occur, and in the absence of an external reductant, all PS I complexes soon switch to the closed RC state and can remain in that state for hours. Addition of 20 mM of sodium ascorbate provides an alternative channel for $P700^+$ reduction through direct electron donation from ascorbate, which occurs with 120 sec kinetics (Savikhin et al., 2001). Addition of 150 μM phenazine methosulfate along with the ascorbate further shortens this reduction time to ∼2 msec (Byrdin et al., 2000), limiting the excitation pulse repetition rate to <500 Hz for static samples. Higher laser pulse repetition rates require the use of spinning samples (Savikhin et al., 1993) or flow cells and allow pulse repetition rates in the range of 1 – 100 kHz, resulting in higher sensitivity of the experimental setup.

III. Ultrafast Spectroscopy of PS I Core Complexes

Figure 4 shows the three-dimensional plot of ΔA measured by optical pump–probe techniques for PS I core complexes from *Synechocystis* sp. PCC 6803 at room temperature as described in detail in (Savikhin et al., 2000). The ΔA signals were inverted to ease visual perception of the three-dimensional surface. In this experiment, PS I trimeric complexes were excited by ∼100 fsec long pulses into the blue edge of Q_y absorption band at 660 nm (Fig. 3), and the absorption changes were probed by a second ∼100 fsec pulse across the entire PS I Q_y absorption band as a function of the time delay between pump-probe pulses. The initial PB signal created by excitation at 660 nm rapidly (<1 psec) transforms into a strong PB maximum at ∼685 nm, which roughly corresponds to the PS I absorption maximum in the steady-state spectrum (Fig. 3) and is an indication of a rapid subpicosecond excitation energy transfer to the most numerous Chl *a* pigments, which absorb in this spectral region. The time-dependent ΔA signals probed at wavelengths above 700 nm maximize ∼3 psec after initial excitation, reflecting much slower energy transfer to red-most Chl pigments. The slow kinetics of the latter process is a natural consequence of a small number of red-most Chls—many single-transfer steps are required before excitation can "find" those

pigments. Excitation equilibration is essentially complete a few psec after excitation and the subsequent changes in ΔA signal reflect the excitation energy trapping by the special pair and the formation of the $P700^+$ state. At times >50 psec after excitation the energy transfer and charge separation processes are essentially complete with an electron residing on phylloquinone A_1, the ΔA signal at its residual value and its spectral shape mimicking that of the ($P700^+ - P700$) difference spectrum shown in Fig. 3. Since phylloquinone and iron sulfur cluster do not absorb in the Q_y region of Chl, the consequent nanosecond electron transfer from A_1 to F_X is not expected to directly induce any changes in the time-dependent ΔA signals. However, noticeable nanosecond-scale changes in ΔA signals have been recently detected (Savikhin et al., 2001) and attributed to an electrochromic shift of the absorption bands of a few antenna Chls in the changing electric field of the extra electron moving from A_1 to F_X (Dashdorj et al., 2004).

The ΔA dynamics measured in pump-probe experiments is a result of tens or even hundreds of individual energy transfer steps (hops). A detailed model of energy transfer would require consideration of $\sim 10^4$ energy transfer channels between all possible excitation donor-acceptor pairs formed from PS I antenna Chls. It would be impossible to extract reliable information about every single-energy transfer step from the measured ΔA profiles. Instead, the kind of data shown in Fig. 4 is often analyzed in terms of decay-associated spectra (DAS). In this analysis, the experimental time-dependent ΔA slices at all wavelengths are fitted globally with a small number of exponential components. The decay times τ_i (or rates $k_i = 1/\tau_i$) for each component are assumed to be wavelength-independent, while the amplitudes A_i are optimized independently for each individual time-dependent ΔA profile and the data is fitted using the following equation:

$$\Delta A(\lambda, t) = \sum_{i=1}^{N} A_i(\lambda) e^{-\frac{t}{\tau_i}}, \qquad (1)$$

where λ is the probe pulse wavelength, and N is the number of decay components used to fit the data. In this model, each decay component is characterized by a unique wavelength dependent DAS $A_i(\lambda)$.

Figure 5 shows DAS obtained by global analysis of the pump–probe data presented in Fig. 4 (Savikhin et al., 2000). A good fit to the time-dependent profiles at all wavelengths could be obtained with a set of only four exponential components with decay times 530 fsec, 2.3 psec, 23.6 psec and a slow >1 nsec component that could not be resolved in the 200 psec time frame of the experiment.

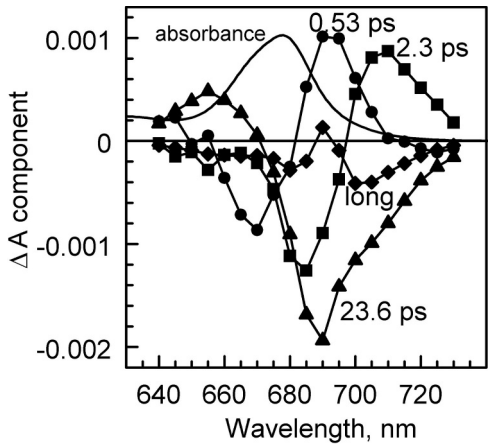

Fig. 5. Decay-associated spectra (DAS) from global analysis of the data shown in Fig. 4: 0.53 psec (•), 2.3 psec (▪), 23.6 psec (▲), and long component (♦). The solid positive line with no symbols represents scaled down steady-state absorption spectrum of PS I for a reference (Savikhin et al., 2000).

A. Excitation Energy Equilibration in the PS I Antenna

1. Subpicosecond Equilibration Among Bulk Chls

The 530 fsec DAS (Fig. 5) has a negative amplitude at ~670 nm, which represents a PB/SE decay and reflects the decrease of excited Chl *a* molecules absorbing at the blue edge of the PS I absorption band. This decay is mirrored by a PB/SE rise occurring at ~690 nm that has the same absolute amplitude and kinetics and represents a simultaneous increase in the number of excited Chl molecules absorbing at longer wavelengths. Such sigmoidal DAS is a typical signature of a downhill energy transfer. Thus, the 530 fsec component arises from spectral equilibration between bulk Chl forms absorbing at ~670 and those absorbing at ~690 nm. A similar subpicosecond energy equilibration component of 360–500 fsec has been revealed by several groups using pump–probe spectroscopy (Melkozernov et al., 2000; Gibasiewicz et al., 2002), as well as fluorescence upconversion (Kennis et al., 2001) for PS I core complexes from *Synechocystis* sp., *Synechococcus elongatus* and *Chlamydomonas reinhardtii*. Recently, Müller et al. (2003) performed a global analysis of the data similar to the one shown in Fig. 4 for PS I core complexes from *C. reinhardtii* in terms of a lifetime density map with the number $N = 70$–100 in Eq. (1) (Croce et al., 2001), and found that it revealed two subpicosecond

components (300 and 800 fsec) in the initial energy equilibration dynamics.

Since the individual energy transfer hops are predicted to be in the order of 100–200 fsec, the observed 300–800 fsec equilibration requires in average 2–8 elementary energy transfer steps. Inability to distinguish a shorter component in isotropic experiments indicates that the first energy transfer step occurs predominantly between Chl molecules with similar optical properties (i.e., with similar absorption and emission spectra) and therefore does not lead to detectable spectral changes in ΔA or fluorescence signals. However, energy transfer between spectrally equivalent molecules with drastic orientations of optical transition moments could be revealed by studying the time-dependent anisotropy $r(t)$ of ΔA or fluorescence signals after exciting a sample using polarized light pulses:

$$r(t) = \frac{S_{||}(t) - S_{\perp}(t)}{S_{||}(t) + 2S_{\perp}(t)}, \qquad (2)$$

where $S_{||}(t)$ and $S_{\perp}(t)$ are ΔA or fluorescence signals detected with light polarization parallel or perpendicular to that of the excitation pulse. Using anisotropic fluorescence upconversion techniques the single step transfer in the PS I core antenna complex was measured to be between 100 and 200 fsec (Du et al., 1993; Kennis et al., 2001). The presence of a similar fast component in pump–probe anisotropies at 680 nm was also indicated in (Savikhin et al., 1999b), but the decay time of that component was not quantified.

2. Picosecond Equilibration with Red Chl Forms

The 2.3 psec DAS (Fig. 5) has a bimodal shape similar to the 530 psec DAS and is attributed to the energy equilibration between the bulk Chls and the "red" Chls absorbing at ∼710 nm. It is no surprise that energy transfer to these Chls takes so long as their number is small and 10–20 single-energy transfer hops are required for the excitation to "find" a red Chl.

The number of red Chl forms in PS I complexes and their spectral positions have been found to be species-dependent (Shubin et al., 1991; Wittmershaus et al., 1992; van der Lee et al., 1993; Gobets et al., 1994, 2001; Pålsson et al., 1996). This leads to a wide spread of picosecond energy equilibration times resolved for PS I complexes in different organisms. There is no clear agreement on the number of red Chl forms in PS I complexes from *Synechocystis* sp. Gobets et al. proposed that there is only one red form absorbing at 706 nm (Gobets and van Grondelle, 2001; Gobets et al., 2001). This is consistent with the single red absorption band observed in low-temperature steady-state absorption spectra of PS I complexes (Rätsep et al., 2000; Gobets et al., 2001) as well as with the single 2.3 psec DAS component (Fig. 5) associated with energy equilibration between bulk and red antenna Chls. A similar single-energy equilibration component of 2–5 psec was reported by several groups using various ultrafast optical techniques (Hastings et al., 1995b; Turconi et al., 1996; Melkozernov et al., 2000; Gobets et al., 2001). However, hole burning experiments performed by Hayes et al. (2000) suggested the presence of two distinct red Chl spectral forms absorbing at 706 and 714 nm, respectively. Savikhin et al. (1999b) also reported the presence of two energy equilibration components (2 and 6.5 psec) in DAS of PS I complexes. However, the latter results were obtained on PS I complexes with closed reaction centers, and the presence of the second energy equilibration component was not confirmed in the later experiments on complexes with open RCs (Savikhin et al., 2000).

A single-energy equilibration component of ∼2 psec was also recently reported for PS I complexes from *C. reinhardtii* (Gibasiewicz et al., 2002; Müller et al., 2003). The absorption spectrum of PS I complexes from *C. reinhardtii* shows the least content of red Chls as compared to the PS I complexes from other species (Gibasiewicz et al., 2002).

PS I complexes from *Synechococcus elongatus* and *Spirulina platensis* each, exhibit two distinct forms of red Chls (Gobets et al., 2001) and as a result two different equilibration components were observed, with lifetimes ∼4 and 10–15 psec (Gobets et al., 2001; Kennis et al., 2001).

The rate of energy equilibration between the bulk antenna Chls and the red Chl forms is clearly dependent on the energy gap between excited states of the antenna and that of the red Chls—larger energy gaps lead to slower equilibration times. The longest equilibration time of 15.1 psec was reported for the *Spirulina platensis* trimeric core complex (Gobets et al., 2001), which contains red Chls absorbing at wavelengths as far as 740 nm. Equilibration with the 708 nm Chl spectral forms in the same complexes occurs within 4.3 psec. This trend is qualitatively consistent with the Förster energy transfer theory, which predicts lower transfer rates as the spectral overlap between donor and acceptor molecules decreases.

B. Excitation Energy Trapping

The shape of the 23.6 psec DAS (Fig. 5) is consistent with the overall decay of a population of excited Chls in PS I antenna caused by excitation trapping at

the reaction center and the formation of $P700^+$ as a result of charge separation. While the 23.6 psec DAS exhibits considerable PB/SE decay amplitude in the red antenna Chl spectral region (>700 nm), it also shows an intense signal at 680–690 nm, overlapping the positive segments of 530 fsec and 2.3 psec DAS. Bulk → red antenna transfers are thus not irreversible; a dynamic equilibrium is reached among the red Chl forms and the bulk antenna. Similar conclusions have been reported by other groups (e.g., Owens et al., 1988; Holzwarth et al., 1990; Werst et al., 1992; Hastings et al., 1995a).

The excitation trapping time was shown to be species-dependent. A trapping time of 20–25 psec was measured for PS I complexes from both *Synechocystis* sp. and *C. reinhardtii* (Hecks et al., 1994; Hastings et al., 1994a; DiMagno et al., 1995; Hastings et al., 1995b; Turconi et al., 1996; Gobets et al., 1998b, Melkozernov et al., 1998a, 2000; Savikhin et al., 2000; Gobets and van Grondelle, 2001; Gobets et al., 2001; Gibasiewicz et al., 2002). A somewhat longer trapping time of 30 psec was reported by Melkozernov et al. (1997) for *C. reinhardtii*. PS I complexes from *Synechococcus elongatus* exhibit trapping times of 30–38 psec (Holzwarth et al., 1993; Byrdin et al., 2000; Gobets et al., 2001; Kennis et al., 2001). The longest energy trapping times of 38–69 psec have been observed in PS I core complexes from *Spirulina platensis* (Karapetyan et al., 1997; Gobets et al., 2001). The increase in energy trapping time in these species correlates with the increased content of red Chl forms combined with the larger spectral shifts of these forms with respect to the energies of the bulk Chls and is consistent with the Förster energy transfer theory.

The validity of the 20–25 psec component assignment to the energy trapping process in *C. reinhardtii* (and perhaps in other species) was recently questioned by Müller et al. (2003). In this work, the authors used a pump–probe technique to obtain data similar to those shown in Fig. 4, but extended the range of probe wavelengths up to 760 nm and analyzed the data in terms of a lifetime density map. The analysis revealed a new component at 6–9 psec which is especially pronounced at wavelengths above 720 nm, and a longer component of ∼20–30 psec similar to the one conventionally assigned to the energy trapping process. The authors proposed that the newly discovered 6–9 psec component is the dominant energy trapping time due to charge separation, and that the longer lifetime represents the consequent electron transfer process, and not trapping as suggested by earlier papers. The new data also suggest that the conventional electron transfer sequence needs to be revised and a new intermediate radical pair state introduced into the kinetic model (see sections "C" and "V" below for further discussion). The new energy/electron transfer kinetic model is intriguing but its validity still needs to be tested by independent experiments.

The DAS of the long >1 nsec component (Fig. 5) represents the $P700^+$ state that is formed as a result of energy trapping and that has a lifetime many orders of magnitude longer than the time window span covered by ultrafast optical experiments. This DAS coincides with a ΔA spectrum measured at a fixed 200 psec delay and is almost superimposable on the steady-state spectrum of the ($P700^+ - P700$) difference spectrum shown in Fig. 3. Slight differences between the steady-state ($P700^+ - P700$) and the ΔA spectrum measured at a fixed 200 psec delay as observed in (Savikhin et al., 2001) were explained by the presence of the electric field of an extra electron, which still resides on the secondary electron acceptor A_1 200 psec after excitation and causes a slight electrochromic shift of the absorption bands of the Chls positioned near A_1 (Dashdorj et al., 2004).

High quantum efficiency of the photosynthetic process implies that the main excitation quenching mechanism in PS I is charge separation initiated when the electronic excitation reaches the special pair. Once charge separation is complete, the special pair switches into its closed (or oxidized) $P700^+$ state and one should expect the excitation lifetime in the antenna to increase substantially (up to the free Chl fluorescence lifetime of ∼4.5 nsec) as the physiological quenching mechanism by charge separation would be blocked. However, extensive evidence suggests that the antenna kinetics are essentially unaffected by the P700 oxidation state (Nuijs et al., 1986; Shuvalov et al., 1986; Owens et al., 1988; Klug et al., 1989; Holzwarth et al., 1993; Turconi et al., 1993; Hastings et al., 1994b; Dorra et al., 1998; Savikhin et al., 2000), and only a slight change in fluorescence quantum yield and fluorescence lifetime for the PS I complex in the closed state was observed (Ikegami, 1976; Telfer et al., 1978; Trissl, 1997; Byrdin et al., 2000). On this basis, the oxidized electron donor $P700^+$ is widely considered to be as good a quencher as the reduced donor P700, although neither the reason nor the physiological significance for this are yet understood. The similarity of antenna kinetics in open and closed PS I complexes opens the unique possibility of comparing the dynamics of excitation in two well-defined redox states of P700, and this strategy has been used by several groups to obtain important information on various aspects of the energy and electron transfer (Shuvalov et al., 1986; Hastings et al., 1994b; White et al., 1996; Byrdin et al., 2000; Savikhin et al., 2001).

Excitation energy trapping by photosynthetic reaction centers is often discussed in terms of "diffusion-limited" or "trap-limited" models (Amesz and Neerken, 2002). In the case of the diffusion-limited model (also called transfer-to-trap-limited model) the rate of trapping is determined only by the rate of diffusion of the excitation energy through antenna pigments to the trap (reaction center), which will only occur if the trap is fully irreversible, i.e., excitation, once transferred to the trap, will not be able to escape back to the antenna. In contrast, the trap-limited model implies that the reaction center is visited by an excitation several times before trapping occurs and the rate of trapping would therefore depend primarily on the trap efficiency.

There is currently no clear agreement on the classification of energy trapping in PS I complexes. On the basis of experimental data and kinetic modeling, several groups argued that the excitation-trapping process in PS I complexes is essentially trap-limited (Holzwarth et al., 1993; Turconi et al., 1993; Hastings et al., 1994a; Kumazaki et al., 1994b; Laible et al., 1994, White et al., 1996; Melkozernov et al., 1997; Beddard, 1998; Dorra et al., 1998). To test the dependence of the energy-trapping rate on the trap efficiency, Melkozernov et al. (1997, 1998b) introduced a site-specific substitution of His-656 residue of PsaB subunit for Asp in the PS I core complexes from *C. reinhardtii*. According to the X-ray structure, the His-656 residue is an immediate ligand to one of the Chls in the special pair and its substitution leads to an increase in redox potential of P700 (Webber et al., 1996) and a change in the P700 photooxidation spectrum. The change in redox potential could cause a decrease in the free energy gap between the primary donor excited state P700* and the primary charge separated state $P700^+A_0^-$, resulting in lower trap efficiency (slower intrinsic charge separation rate). The authors observed the doubling of trapping time in the mutant (~65 psec) as compared to that in wild type PS I, which is consistent with the trap-limited model of energy transfer. However, due to spectral congestion, direct measurement of the intrinsic charge-separation rate in PS I is a challenging task, and one cannot exclude the possibility that the slow excitation trapping rate observed in the mutant may have been caused by the decreased spectral overlap of the primary electron donor P700 with the surrounding antenna.

Back-transfer of excitation from P700* to the antenna is also an indicator of a trap-limited process and has been reported by several groups. White et al. (1996) excited PS I complexes from higher plants at 708 nm in an attempt to create the P700* state directly and observe the consequent formation of $P700^+$, but were forced to conclude that energy transfer from P700* to the antenna is faster than the intrinsic primary charge separation time, which was estimated to be ~1.3 psec. Kumazaki et al. (1998, 2001) studied PS I complexes from higher plants containing only 12–13 Chls per special pair, with the majority of the antenna Chls removed chemically. Both fluorescence upconversion and absorption pump–probe experiments indicated that at least half of the excitations created initially on the special pair escape into the remaining pool of antenna Chls instead of being trapped by the charge separation process. The intrinsic charge-separation time was estimated to be ~1.3–2 psec, while the excitation back-transfer component of ~0.3 psec was observed in fluorescence upconversion experiments (Kumazaki et al., 1998), and an even shorter ~0.1 psec process was detected in the later study using absorption pump–probe techniques (Kumazaki et al., 2001). However, the latter 0.l psec process could be caused by coherent nuclear vibration of P700*, and the presented pump–probe data was in general more consistent with the back-transfer rate being almost equal to the intrinsic charge separation rate. It should be noted here that chemically treated PS I complexes are not equivalent to native complexes, as the removal of a significant number of antenna Chls would necessarily alter the dynamics of the energy equilibration process between antenna Chls and the special pair and may also lead to structural damage of these pigment–protein complexes.

The independence of the effective excitation trapping time on the excitation wavelength (see, e.g., Pålsson et al., 1998; Melkozernov et al., 2000) is also indicative of the trap-limited description of excitation dynamics in PS I.

An alternative transfer-to-trap-limited model of energy trapping in PS I was proposed by several groups (van Grondelle et al., 1994; Valkunas et al., 1995a; Croce et al., 1996; Jennings et al., 1997; Trissl, 1997; Gobets et al., 1998a,b; Pålsson et al., 1998). The transfer-to-trap-limited model implies that while Boltzmann equilibration within the antenna is reached, there is no equilibrium between the antenna and the RC. As a criterion for the Boltzmann equilibrium, the so-called Stepanov–Kennard relation was applied to study the extent of thermal equilibration in PS I-200 particles from higher plants (Croce et al., 1996; Jennings et al., 1997). It was found that the fluorescence yield observed in the experiment was lower than calculated according to the Stepanov–Kennard relation. This was interpreted as an indication that the excitation is trapped by the RC faster than excitation equilibration can be established. However, care should be taken when applying these

results to the core complexes as the PS I-200 particles still contain the outer light-harvesting antenna complex (LHCI), which slows down the overall trapping process. Pålsson et al. (1998) used a similar thermalization approach to study PS I core complexes from *Synechococcus elongatus* and suggested that at low temperatures the rate of primary charge separation is much faster than the back-transfer of the excitation energy from P700* to the neighboring antenna pigments. They also proposed that at room temperature ~50% of photochemical trapping might occur from the red pigments to P700, in which case the latter energy transfer process would represent a bottleneck process. Gobets et al. (1998a,b) modeled time-resolved fluorescence data obtained for PS I core complexes from *Synechococcus elongatus* and *Synechocystis* sp. and suggested that the slow energy transfer from the red pigments located on the periphery of the complex limits the trapping.

Drastically different conclusions reached by various groups on the classification of energy transfer process in PS I complexes are based on essentially similar experimental data. The key factor preventing unanimous agreement in the interpretation of the experimental data is the complexity of the system. Even though the structure of PS I has been determined to high precision, the spectral positions of most of the Chls constituting the PS I antenna are unknown and modeling includes a lot of guessing. Moreover, the measured optical signals are caused by a mixture of many energy (electron) transfer steps, occurring concurrently, and extracting individual (intrinsic) kinetic parameters becomes tricky. It is very possible that energy trapping in PS I is neither of the extreme cases discussed above, but rather an intermediate case where both excitation energy diffusion from the antenna to the special pair and the intrinsic charge separation rate influence the energy trapping in a balanced way (Trinkunas and Holzwarth, 1996; Holzwarth et al., 1998; Karapetyan et al., 1999; Byrdin et al., 2000, 2002).

Trinkunas and Holzwarth (1996) analyzed the available experimental fluorescence data using a genetic algorithm and various kinetic models and reported that the data were inconsistent with both purely transfer-to-trap- and purely trap-limited models. For PS I complexes from *Spirulina platensis*, a new model was suggested with nearly trap-limited excitation transfer from bulk antenna to P700 and a diffusion-limited excitation transfer from the red Chl pools via the bulk antenna (Holzwarth et al., 1998; Karapetyan et al., 1999).

Byrdin et al. (2000) used the latest 2.5 Å structure of PS I (Jordan et al., 2001) to build a detailed model that would reproduce static optical properties of PS I complexes from *Synechococcus elongatus* (steady-state absorption, linear, and circular dichroism) along with excitation transfer and trapping dynamics observed experimentally. The model predicts that electronic light excitation visits P700 an average of six times before being trapped photochemically and creating a charge separated state. Therefore, the overall energy trapping rate must depend on the trap efficiency. Indeed, the two-fold increase or decrease in the intrinsic charge separation rate in respect to its original value of 0.87 psec^{-1} resulted in 23 and 56 psec trapping lifetimes instead of the original 34 psec. On the other hand, similar variations in the Förster parameter R_0, which governs excitation energy transfer rate between Chls, rendered lifetimes of 28 and 45 psec. The authors concluded that the antenna excited state decay lifetime (and trapping) depended on all key parameters of the model—the intrinsic charge separation rate, the transfer-to-the trap rate, and the transfer rate between individual antenna Chls—and that the excited state dynamics is neither pure trap-limited, nor pure transfer-to-trap-limited.

C. Charge Separation and Electron Transfer Kinetics

When discussing the dynamics of charge separation and consequent electron transfer processes in a photosynthetic system, it is important to clearly differentiate between the "effective" transfer rates and the "intrinsic" rate constants. To avoid possible ambiguity, we will adhere to the terminology defined in (Gatzen et al., 1996; Müller et al., 2003). The term "intrinsic rate constant for electron transfer" will be used exclusively to denote the kinetic rate of an individual electron transfer step from a particular electron donor molecule to a particular acceptor molecule in the assumption that all other transfer processes are blocked. The "effective rate constant" (sometimes referred to as "apparent rate constant") is defined as the rate at which a certain redox state is populated (or depopulated). Thus, the energy trapping time of 20–65 psec observed in experiments as the decay of antenna excitation is equivalent to the *effective* charge separation time (time = 1/rate), since excitation trapping leads to the creation of the radical pair(s) and is a consequence of many individual energy transfer steps followed by a single electron transfer step. In contrast, the *intrinsic* charge separation time in PS I represents the kinetics of charge separation in the case when excitation is created directly on P700 and back-transfer from P700 to the antenna, as well as charge recombination are blocked. Since for the PS I complex the described conditions cannot be achieved, the intrinsic

rate constant cannot be directly observed in experiment and is usually obtained via model simulations.

There is unanimous agreement that the intrinsic charge separation rate in PS I RC is much faster than the observed effective excitation trapping rate. Most of the studies put the intrinsic charge separation step in PS I RC in the 0.5–3 psec time range, and the consequent electron transfer from primary electron acceptor A_0 to the secondary electron acceptor A_1 is believed to occur in 10–50 psec (Brettel and Leibl, 2001). However, the precise measurement of these important kinetic parameters presents a challenging problem. Isolation of the RC cofactors from PS I is impossible as the two main protein subunits PsaA and PsaB that coordinate the cofactors also bind most of the antenna Chls. The presence of antenna pigments and spectral congestion among reaction center cofactors precludes selective excitation of P700 and complicates the isolation of the optical signals arising from the electron transfer process from the signals stemming from the excitation energy transfer.

Kumazaki et al. (1994a,b, 2001) tried to minimize the contribution of antenna processes to the measured transient absorption and fluorescence signals by chemical treatment of PS I complexes from spinach that removed most of the antenna Chls from complexes, leaving only 12–14 Chls per P700. Due to the small amount of antenna Chls, preferential excitation of P700 became possible. The authors found that the effective primary charge separation kinetics in these complexes could be described by two components of equal amplitudes with time constants of 0.8 ± 0.1 and 9 ± 1 psec (Kumazaki et al., 2001). The short 0.8 psec component was ascribed to the formation of the charge separated state generated directly from the initially excited P700*, and the relatively slow 9 psec component was assumed to stem from excitations which escaped from P700* to the surrounding pigments and were recaptured at later times. A kinetic model revealed that the observed data could be reproduced with an intrinsic charge separation time of 0.5–0.8 psec.

Several groups (Nuijs et al., 1986; Shuvalov et al., 1986; Wasielewski et al., 1987; Hastings et al., 1994b; Kumazaki et al., 1994b; White et al., 1996; Savikhin et al., 2001) proposed a strategy for isolating the reaction center kinetics by obtaining time-resolved absorption difference profiles for PS I core complexes with open and closed reaction centers. Since extensive experimental evidence suggests that the antenna kinetics are unaffected by the P700 oxidation state, the difference $\Delta\Delta A$ between absorption difference profiles for open and closed RCs ($\Delta\Delta A = \Delta A_{\text{openRC}} - \Delta A_{\text{closedRC}}$) should isolate the electron transfer processes, since they occur only in complexes with open RCs. Hastings et al. (1994b) applied this method to study PS I complexes from *Synechocystis* sp. The experimental $\Delta\Delta A$ profiles probed at 686 nm exhibited an initial PB rise feature of ~4 psec followed by ~21 psec PB decay. This probe wavelength corresponds to the maximum position of the A_0 absorption band, and the observed kinetics were attributed to the formation and decay of the A_0^- state. The authors concluded that the ~4 psec rise represented the effective energy-trapping time, which was significantly shortened as a result of annihilation caused by the use of high-excitation pulse intensities, and that the 21 psec component characterized the intrinsic rate of the $A_0 \rightarrow A_1$ electron transfer step. Savikhin et al. (2001) have further extended this method and studied annihilation-free $\Delta\Delta A$ profiles probed in a wide spectral range with significantly lowered noise levels (Fig. 6). Assuming that all of the antenna kinetics were canceled by the (open-closed) subtraction procedure, the shown $\Delta\Delta A$ profiles should reflect the formation and decay dynamics of only three states:

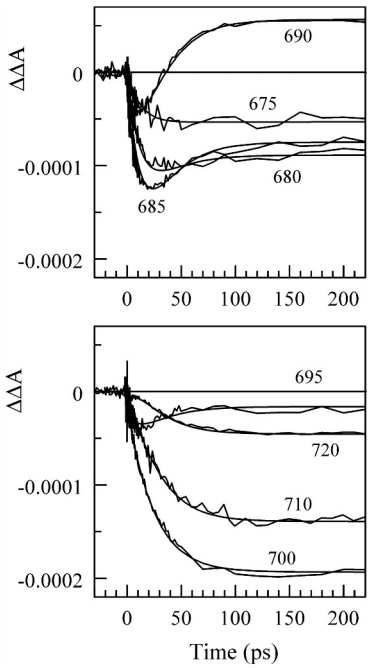

Fig. 6. Time-resolved (open-closed) absorption difference profiles for PS I complexes from *Synechocystis* sp. excited at 660 nm and probed at specified wavelengths. Noisy curves are experimental. Smooth curves are the results of global fit with only two free parameters – intrinsic charge separation and first electron transfer step times; all amplitudes were fixed as described in (Savikhin et al., 2001).

$P700^*A_0A_1$, $P700^+A_0^-A_1$, and $P700^+A_0A_1^-$. Using a simple sequential model of electron transfer, all of the curves shown in Fig. 6 were fitted globally with only two free parameters, resulting in the intrinsic times for charge separation and the following $A_0 \rightarrow A_1$ electron transfer step of 1.3 and 13 psec, respectively. White et al. (1996) applied a similar approach to study dynamics of electron transfer process in PS I complexes from spinach. Using simple models of energy migration, the intrinsic rates of charge separation and primary electron transfer step were estimated to be 1.4 and 20 psec, respectively. It was also found that even when the femtosecond pulses were tuned to preferentially excite P700, only a small fraction of the initially excited P700* led to the charge separated state while the rest of the excitations escaped to the antenna.

The formation and decay kinetics of A_1^- can be monitored directly in its broad near-UV absorption band around 380–390 nm (Brettel et al., 1986; Brettel, 1988; Lüneberg et al., 1994; Brettel and Vos, 1999). At this probe wavelength, Brettel et al. (1999) observed ΔA transient for *Synechocystis* sp., which could be described by two exponentials with time constants of 7 and 28 psec. The shorter component was attributed to the antenna processes presumably accelerated by an annihilation artifact due to high excitation levels, and the longer component was interpreted as the intrinsic time of $A_0 \rightarrow A_1$ electron transfer step. However, the observed build-up of the A_1^- state was probably delayed by the preceding antenna equilibration and charge separation steps and the reported 28 psec time is likely to be an overestimate. While annihilation phenomenon shortens the antenna excitation lifetime, it also precludes precise measurement of the effective trapping time, since the observed antenna excitation decay is not caused by merely charge separation process anymore. To avoid complications arising from annihilation processes, we performed a similar experiment under low excitation levels. Figure 7A (upper line) shows ΔA kinetics probed at 390 nm after exciting open PS I complexes at 660 nm (N. Dashdorj and S. Savikhin, unpublished). The measured annihilation-free pump–probe profile could be described with a single PB exponent with a time constant of 30 ± 3 psec followed by a non-decaying positive component. In the absence of annihilation, the (effective) trapping that precedes $A_0 \rightarrow A_1$ electron transfer step occurs in 23 psec, which implies that the intrinsic $A_0 \rightarrow A_1$ transfer step is significantly faster than the measured 30 psec time constant. Moreover, the 390 nm signal is initially dominated by the photobleaching of the antenna Chl *a* pigments, and the formation and decay of the reduced A_0^- state may also

Author: Please add "Brettel et al., 1999" to the list.

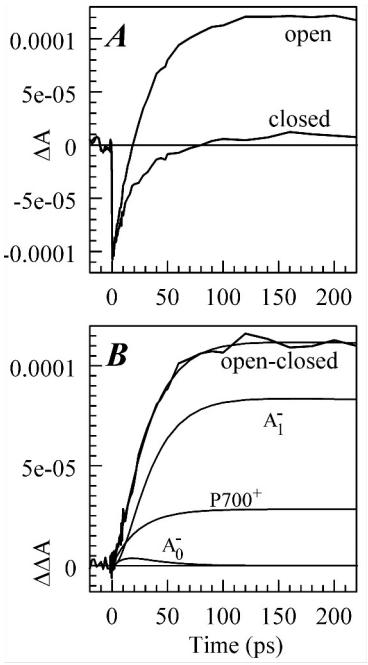

Fig. 7. Time-resolved absorption difference profiles for WT PS I complexes from *Synechocystis* sp. excited at 660 nm and probed at 390 nm. (A) ΔA profiles obtained for PS I complexes with open and closed RCs. (B) Time-resolved (open-closed) absorption difference profile, and the optimized fit to it. Signal contributions due to formation of $P700^+$, A_0^-, and A_1^- are also shown.

contribute to the signal. To simplify the analysis, the $\Delta\Delta A$ profile was obtained by subtraction of the ΔA profile for the closed RC from that for the open RC (Fig. 7B). As a result, the early time negative component that stems from excited antenna pigments was canceled (Savikhin et al., 2001), and the resulting profile was fitted using a simple sequential electron transfer model:

$$(\text{Antenna} + P700)^* \xrightarrow{\tau_1} (P700^+A_0^-A_1) \xrightarrow{\tau_2} (P700^+A_0A_1^-)$$

The effective charge separation time τ_1 was fixed at 23 psec (the measured antenna excitation decay time), and a good fit to the data could be obtained with the intrinsic electron transfer time τ_2 varied in the range of 8–15 psec. Similar τ_2 could be obtained by fitting the original unprocessed pump–probe profile for open PS I complexes (Fig. 7A, upper line) and modeling the uncanceled signal contribution due to the antenna excitation decay by a single 23 psec PB component.

The build-up of the positive ΔA signal in the 380–390 nm region upon the formation of $P700^+A_1^-$

observed by Brettel et al. (1999) and our group is, however, not consistent with the picosecond transient absorption measurements by Mi et al. (1999), who reported that the ($P700^+A_1^- - P700A_1$) difference spectrum for *Synechocystis* sp. is negative in this spectral range. The source of this discrepancy is not clear.

A different electron transfer scenario was proposed recently by Müller et al. (2003) on the basis of pump-probe data obtained after exciting PS I complexes from *C. reinhardtii* at 670 and 700 nm. The number of "red" pigments in PS I complexes from these species is small and 700 nm pump pulses excite predominantly P700 dimer directly, while the 670 nm excitation represents the contrasting case when all of the electronic excitations are initially created in the antenna. By comparing pump–probe data measured in these different excitation regimes and analyzing the data in terms of species-associated difference spectra, the authors found that the experimental results could be explained only if one additional radical pair was introduced to the conventional scheme of electron transfer. According to the most probable scenario proposed in the paper, the intrinsic charge separation time is 2.9 psec, which is combined with the backward recombination process with intrinsic time of ~40 psec. Primary charge separation is followed by two fast electron transfer steps with intrinsic times of 13 and 35 psec, respectively, which lead to the formation of $P700^+A_1^-$. The first 13 psec electron transfer step is in good agreement with the result reported by Savikhin et al. (2001), although according to the latter group, the 13 psec transfer step already leads to the formation of $P700^+A_1^-$. Müller et al. (2003) proposed an intriguing possibility that the additional radical pair involves the accessory pigment A_{acc} and that the primary charge separated state may be not $P700^+A_0^-$, but $P700^+A_{acc}^-$ or $A_{acc}^+A_0^-$ (A_{acc} is used to denote one of the accessory Chls, Fig. 2). Formation of the former charge separation state would be reminiscent of the main electron transfer mechanism in the bacterial RC (Woodbury and Allen, 1995).

D. Directionality of Electron Transfer

The presence of two highly symmetrical branches in the RC of PS I raises the question of directionality of the ET in this complex. Evidence for bidirectional ET has mainly been obtained for PS I of eukaryotes such as the alga *Chlorella sorokiniana* (Joliot and Joliot, 1999) and *C. reinhardtii* (Boudreaux et al., 2001; Fairclough et al., 2001; Guergova-Kuras et al., 2001; Muhiuddin et al., 2001), while evidence for more asymmetric electron transfer in PS I has been reported for prokaryotes such as the cyanobacterium *Synechocystis* sp. PCC 6803 (Golbeck et al., 2001; Xu et al., 2003a,b). The conclusions about the electron transfer pathway in PS I are based primarily on studies involving specific mutations around the respective phylloquinone (A_1) binding sites on the PsaA and PsaB polypeptides (Joliot and Joliot, 1999; Boudreaux et al., 2001; Guergova-Kuras et al., 2001; Muhiuddin et al., 2001). The advantage of these mutations is that the spectral and functional changes they induce are so subtle that they do not influence the charge separation. The disadvantage is that the subtle nature of the changes induced by the mutations leaves some ambiguity in the interpretation of the spectral data. Moreover, these experiments have been focusing primarily on the measurements of the changes in the ET kinetics (optical and EPR), which reflect relatively slow nanosecond electron transfer from the A_1 to F_X. In this case, the electron acceptor is common for both branches and the mutational changes around A_1 (which is close to F_X) in one branch can influence the properties of F_X and through that ET kinetics through the other branch.

Recently, Cohen et al. (2004) constructed identical mutations in both the PsaA-side and the PsaB-side at the corresponding A_0 sites modifying the properties of the primary electron acceptor in PS I complexes from *Synechocystis* sp.PCC 6803. In particular, the methionines in $M688_{PsaA}$ or $M668_{PsaB}$ positions were replaced by leucine or asparagine. These methionines are proposed to provide the axial ligands to the respective Mg^{2+} ions of the two A_0 chlorophylls and a change in the ligand would be expected to alter the mid point potential of the A_0^-/A_0 redox pair, causing changes in electron transfer dynamics. Nanosecond optical and EPR experiments revealed significant differences between the PsaA-branch and the PsaB-branch mutants which were more consistent with the assumption that ET occurs primarily along A-branch of the RC (Cohen et al., 2004). These measurements, however, did not have time resolution sufficient to detect changes in the first two electron transfer steps, which directly involve A_0 and would be naturally affected by such point mutations. We have recently performed a series of ultrafast pump–probe experiments on the same samples and supported their findings (Dashdorj et al., 2005). Figures 8A,B show the A_1^- formation dynamics probed at 390 nm for PS I complexes with point mutations in PsaA- and PsaB-branch, respectively, along with the analogous data obtained in native complexes shown previously in Fig. 7. Mutations in PsaB-branch had essentially no effect on electron transfer, while the $A_0 \rightarrow A_1$ electron transfer in PsaA-branch mutants increased

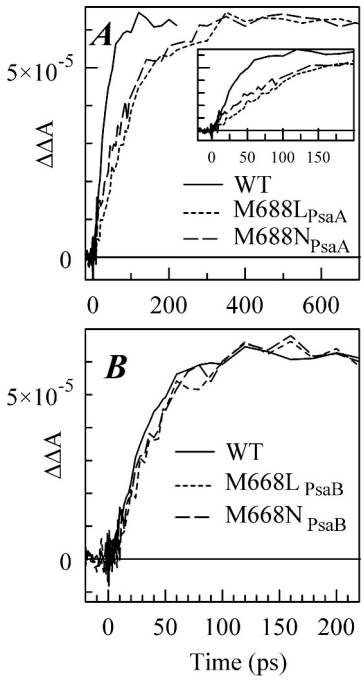

Fig. 8. Time-resolved (open-closed) absorption difference profiles for WT, M668L_{PsaB}, and M668N_{PsaB} mutants (A), and for WT, M688L_{PsaA} and M688N_{PsaA} mutants (B). All samples were excited at 660 nm and absorption differences were probed at 390 nm.

to ∼100 psec. The presented data suggests that in PS I complexes from *Synechocystis* sp., electron transfer preferably occurs along the PsaA-branch of the RC, and that the function of the primary electron acceptor A_0 is served by Chl denoted as eC-A_3 in Fig. 2.

Different results were reported by Ramesh et al. (2004) for PS I complexes from *C. reinhardtii.* These authors introduced branch-specific mutations replacing the methionine residue that provides axial bond to eC-A_3 in the PsaA or eC-B_3 in the PsaB-branch by histidine (see Fig. 2). According to ultrafast pump–probe absorption difference data, the long-lived ($A_0^- - A_0$) difference signal accumulates at ∼686 nm in complexes with mutation in either branch, demonstrating that electron transfer between A_0^- and A_1 is blocked or significantly slowed down by this substitution and suggesting that electron transfer occurs along both branches concurrently. These findings support earlier conclusions on bidirectionality of electron transfer in *C. reinhardtii* (Boudreaux et al., 2001; Fairclough et al., 2001; Guergova-Kuras et al., 2001; Muhiuddin et al., 2001).

The contrasting results on directionality of electron transfer may indicate that the electron transfer path in PS I is species-dependent and that relatively small changes in PS I protein structure expected for these organisms may have a significant impact on the details of the electron transfer process.

E. Excitonic Coupling in a PS I Core Complex

The close proximity of pigments to each other in PS I leads to strong excitonic coupling between nearby Chls, altering optical properties of single pigment transitions and further complicating the analysis of transient signals. Excitonic states can be recognized by their distinct signatures in ΔA spectra. Upon excitation into an excitonic band, the early time ΔA spectra typically spread far beyond the excitation pulse bandwidth and exhibit rich spectral structure. Moreover, while the initial anisotropy $r(0)$ of ΔA signals following excitation of an ensemble of single molecules is typically close to 0.4, the $r(0)$ values of excitonic transitions depend strongly on wavelength and may take any value (see the underlying theory in Savikhin et al., 1999a).

It is widely accepted that the close spacing of the two Chls forming P700 leads to excitonic coupling and results in a broad absorption band observed at ∼700 nm in ($P700^+ - P700$) spectra (Fig. 3). Gibasiewicz et al. (2002) resolved a highly structured instant ΔA spectrum upon exciting PS I complexes from *C. reinhardtii* at 10 K with 700 nm light pulses that targeted primarily the P700 optical transition. They observed four positive bands accompanied by four negative bands spread over the range of 634–695 nm, far beyond the spectral width of the excitation pulse. The quantity of the observed bands indicated that excitonic coupling spreads over more than just the two pigments forming P700. The observed ΔA spectrum was explained in terms of an excitonic system consisting of all six pigments constituting the RC. For such a system, one should expect six excitonic PB bands combined with 15 excitonic ESA bands and one SE band (Savikhin et al., 1999a). The lower number of the observed features may stem from the low intensity of some of the excitonic transitions and/or overlapping bands.

Savikhin et al. (1999b, 2000) studied PS I complexes from *Synechocystis* sp. by means of the pump–probe technique. Upon exciting complexes at 710 or 720 nm they observed "anomalous" negative initial anisotropies $r(0) \sim -0.5$, which suggest the presence of mutually orthogonally polarized components near ∼718 and 680 nm, suggesting that the red-most Chl antenna transition(s) arise from two (or more) strongly coupled Chls. This interpretation is in line with hole-burning experiments (Hayes et al., 2000;

Rätsep et al., 2000; Zazubovich et al., 2002), Stark effect measurements (Frese et al., 2002), and fluorescence line-narrowing studies (Gobets et al., 1994). Several strongly coupled pairs have been proposed to serve as the red-most pigments based on the available X-ray structure (Jordan et al., 2001; Byrdin et al., 2002; Damjanovic et al., 2002; Dashdorj et al., 2004).

IV. Ultrafast Spectroscopy of PS I–LHCI Supercomplexes

In plants and green algae, the PS I core complex is surrounded by the Chl *a*/*b* containing light-harvesting complex (LHC) I that serves as peripheral antenna, increasing the efficiency of the system by capturing additional light and guiding its energy to the PS I core complex antenna (Gobets and van Grondelle, 2001; Melkozernov, 2001; Ben-Shem et al., 2003). The recent 4.4 Å resolution X-ray structure of the PS I–LHCI from pea (Ben-Shem et al., 2003) shows a layer of four evenly spaced monomeric LHCI proteins (Lhca1, 2, 3, and 4) which are in structural contact with PS I and increase the antenna size to 167 Chls per RC (see Nelson and Ben-Shem, this volume, Chapter 7). The structural details of PS I–LHCI supercomplex from green algae are still unknown, but the available low-resolution electron microscopy of *C. reinhardtii* predicts binding of 11–14 Lhca proteins (Germano et al., 2002; Kargul et al., 2003), resulting in an even larger antenna size.

The presence of additional antenna components in PS I–LHCI supercomplexes results in significant heterogeneity of the Chl excitation dynamics and leads to a slower energy trapping process but does not affect the consequent electron-transfer steps (van Grondelle et al., 1994; Pålsson et al., 1995; Croce et al., 2000; Melkozernov, 2001; Melkozernov et al., 2004). Croce et al. (2000) used a single-photon counting technique to resolve the fluorescence dynamics of intact PS I–LHCI supercomplexes from higher plants (PS I-200 particles) and found that excitation trapping could be described by two components of 57 and 130 psec. A single 67 psec excitation trapping component in PS I-200 complexes was measured by Gobets et al. (2001) using a synchroscan streak camera. In comparison, excitation trapping in plant core complexes that miss the peripheral antenna is much faster and occurs in 22 psec (Gobets and van Grondelle, 2001). A similar effect was reported by Melkozernov et al. (2004), who studied excitation transfer and trapping dynamics in PS I–LHCI supercomplexes from a green alga *C. reinhardtii* by means of pump–probe and fluorescence spectroscopy. The excitation trapping was found to be biphasic, with the shorter 25 ± 3 psec component ascribed to photochemical trapping in the PS I core antenna, and the longer 104 ± 20 psec component attributed to excitation trapping occurring from the peripheral LHCI complexes. The slow 104 psec process suggests the presence of a slow energy-transfer pathway from the LHCI to the PS I core and indicates that excitation trapping from the peripheral antenna is diffusion-limited.

The energy equilibration and trapping processes in PS I–LHCI supercomplexes are addressed in more detail by Karapetyan et al., this volume, Chapter 13.

V. Concluding Remarks

The extensive experimental data on the dynamics of energy and electron transfer in PS I core complexes is summarized in the compartment model shown in Fig. 9A. Here, the effective (observable) transfer/equilibration times are labeled in italic, and the intrinsic transfer times are labeled in bold. The antenna is represented as three pools of Chls that are grouped by their Q_y optical transition energies and absorb at ~660, ~680, and >705 nm, respectively. Introduction of three pools is necessary to account for two energy equilibration processes observable in ultrafast optical experiments—or the 300–800 fsec equilibration between Chls absorbing at ~660 and Chls absorbing at ~680 nm, and 2–5 psec equilibration with the small pool of red Chls absorbing at >705 nm. The energy transfer rates from the antenna pigments to the special pair P700 and possible back-transfer rates are model dependent. In the case of a diffusion-limited transfer model, the back-transfer rate from P700 to antenna is negligible and the forward energy transfer rate is essentially equal to the observable effective energy-trapping time. In the case of a trap-limited model, the choice of a unique pair of forward and back-transfer rates is not straightforward since many combinations of forward and backward transfer rates can reproduce the effective excitation trapping rate observed experimentally. The model depicted in Fig. 9A represents a conventional sequence of electron transfer steps, which involves two radical pairs ($P700^+A_0^-\ A_1F_X$) and ($P700^+A_0A_1^-\ F_X$) that precede the relatively slow nanosecond formation of the ($P700^+A_0A_1F_X^-$) state. Figure 9B shows one of the alternative compartment models proposed recently by Müller et al. (2003), which models antenna with only two pools of pigments but adds one more intermediate radical pair to the conventional sequence of electron transfer. The exact nature of the additional radical pair

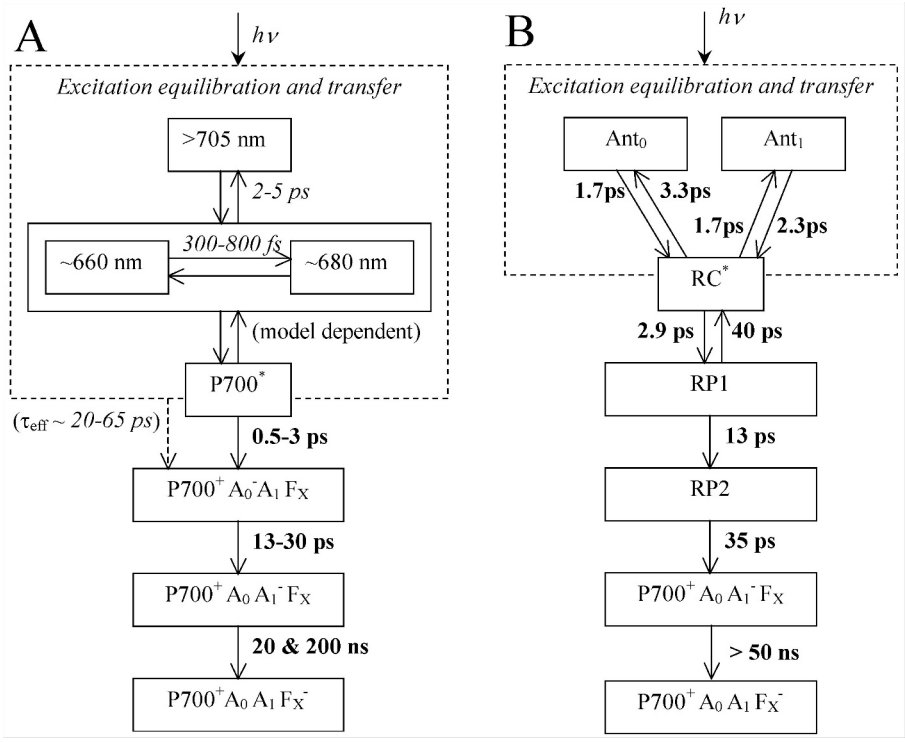

Fig. 9. (A) Compartment model of energy and electron transfer in PS I core complexes consistent with the data presented in Figs. 4 and 6. (B) One of the alternative compartment models with an extra radical pair proposed by Müller et al. (2003). The intrinsic transfer times are printed using bold typeface. In scheme (B) the original transfer rates were converted to lifetimes (time = 1/rate) for easier comparison.

is not known, but it would most probably involve oxidation or reduction of the accessory Chl.

The compartment models shown in Fig. 9 do not exhaust all possible arrangements used to model the results of ultrafast optical experiments (see, e.g., White et al., 1996; Gobets et al., 2001; Kumazaki et al., 2001; Müller et al., 2003). However, while compartment models of excitation transfer and equilibration significantly simplify the analysis of the observable kinetics, they are inherently only approximations of the real processes. Dividing antenna Chls into pools based on their spectroscopic properties ignores the fact that Chls belonging to different spectral pools do not form spatially separated groups but are most probably randomly mixed (interlaced), forming a strongly coupled net of pigments. Availability of high resolution X-ray structure of PS I opens the excellent possibility of building a complete model of energy transfer in this complex that would include excitation transfer between all antenna pigments, or between all excitonic states formed by all strongly coupled antenna pigments (see, e.g., Byrdin et al., 2002). However, for precise simulations, these models require knowledge of Q_y transition energies of each of the pigments in the antenna. Due to spectral congestion, the transition energies of most of the antenna pigments are not accessible in optical experiments—to date, only spectra of P700 and A_0 have been measured reliably. Alternatively, the spectral positions of Chls in antenna could be predicted by performing molecular simulations based on the known local protein structure around each pigment (Damjanovic et al., 2002), though the results of such calculations are difficult to verify.

Acknowledgments

I gratefully thank the following coworkers with whom some of the work discussed in this chapter has been developed: Dr. Walter S. Struve, Dr. Parag R. Chitnis, Dr. Wu Xu, Dr. Peter Martinsson, Dr. John H. Golbeck, and Naranbaatar Dashdorj. I am also indebted to Dr. Stephen M. Durbin for useful comments on the manuscript. Some of the work reported in this chapter was supported by Purdue Research Foundation grant 6903680.

References

Amesz J and Neerken S (2002) Excitation energy trapping in anoxygenic photosynthetic bacteria. Photosynth Res 73: 73–81

Beddard GS (1998) Excitations and excitons in photosystem I. Phil Trans R Soc London 356: 421–448

Ben-Shem A, Frolow F and Nelson N (2003) Crystal structure of plant photosystem I. Nature 426: 630–635

Boudreaux B, MacMillan F, Teutloff C, Agalarov R, Gu F, Grimaldi S, Bittl R, Brettel K and Redding K (2001) Mutations in both sides of the photosystem I reaction center identify the phylloquinone observed by electron paramagnetic resonance spectroscopy. J Biol Chem 276: 37299–37306

Brettel K (1988) Electron transfer from A_1^- to an iron–sulfur center with $t_{1/2} = 200$ ns at room temperature in photosystem I. Characterization by absorption spectroscopy. FEBS Lett 239: 93–98

Brettel K (1997) Electron transfer and arrangement of the redox cofactors in photosystem I. Biochim Biophys Acta 1318: 322–373

Brettel K and Leibl W (2001) Electron transfer in photosystem I. Biochim Biophys Acta 1507: 100–114

Brettel K and Vos MH (1999) Spectroscopic resolution of the picosecond reduction kinetics of the secondary electron acceptor A_1 in photosystem I. FEBS Lett 447: 315–317

Brettel K, Sétif P and Mathis P (1986) Flash-induced absorption changes in photosystem I at low temperature: evidence that the electron acceptor A_1 is vitamin K_1. FEBS Lett 203: 220–224

Byrdin M, Rimke I, Schlodder E, Stehlik D and Roelofs TA (2000) Decay kinetics and quantum yields of fluorescence in photosystem I from *Synechococcus elongatus* with P700 in the reduced and oxidized state: are the kinetics of excited state decay trap-limited or transfer-limited? Biophys J 79: 992–1007

Byrdin M, Jordan P, Krauß N, Fromme P, Stehlik D and Schlodder E (2002) Light harvesting in photosystem I: modeling based on the 2.5-Å structure of photosystem I from *Synechococcus elongatus*. Biophys J 83: 433–457

Cohen R, Shen G, Golbeck JH, Xu W, Chitnis PR, Valieva A, van der Est A, Pushkar J and Stehlik D (2004) Evidence for asymmetric electron transfer in cyanobacterial photosystem I: analysis of a methionine to leucine mutation of the ligand to the primary electron acceptor A_0. Biophys J 43: 4741–4754

Croce R, Zucchelli G, Garlaschi FM, Bassi R and Jennings RC (1996) Excited state equilibration in the photosystem I light harvesting complex: P700 is almost isoenergetic with its antenna. Biochemistry 35: 8572–8579

Croce R, Dorra D, Holzwarth AR and Jennings RC (2000) Fluorescence decay and spectral evolution in intact photosystem I of higher plants. Biochemistry 39: 6341–6348

Croce R, Müller MG, Bassi R and Holzwarth AR (2001) Carotenoid-to-chlorophyll energy transfer in recombinant major light-harvesting complex (LHC II) of higher plants. I. Femtosecond transient absorption measurements. Biophys J 80: 901–915

Damjanovic A, Vaswani HM, Fromme P and Fleming GR (2002) Chlorophyll excitations in photosystem I of *Synechococcus elongatus*. J Phys Chem B 106: 10251–10262

Dashdorj N, Xu W, Martinsson P, Chitnis PR and Savikhin S (2004) Electrochromic shift of chlorophyll absorption in photosystem I from *Synechocystis* sp. PCC 6803: a probe of optical and dielectric properties around the secondary electron acceptor. Biophys J 86: 3121–3130

Dashdorj N, Wu W, Cohen RO, Golbeck JH and Savikhin S (2005) Asymmetric electron transfer in cyanobacterial Photosytem I: charge separation and secondary electron transfer dynamics in mutations near the primary electron acceptor A_0. Biophys J 88: 1238–1249

Diaz-Quintana A, Leibl W, Bottin W and Sétif P (1998) Electron transfer in photosystem I reaction centers follows a linear pathway in which iron–sulfur cluster F_B is the immediate electron donor to soluble ferredoxin. Biochemistry 37: 3429–3439

DiMagno L, Chan C-K, Jia Y, Lang MJ, Newman JR, Mets L, Fleming GR and Haselkorn R (1995) Energy transfer and trapping in photosystem I reaction centers from cyanobacteria. Proc Natl Acad Sci USA 92: 2715–2719

Dorra D, Fromme P, Karapetyan NV and Holzwarth AR (1998) Fluorescence kinetics of photosystem I: multiple fluorescence components. In: Garab G (ed) Photosynthesis: Mechanisms and Effects, pp 587–590. Kluwer Academic Publishers, Dordrecht, The Netherlands

Du M, Xie X, Jia Y, Mets L and Fleming GR (1993) Direct observation of ultrafast energy transfer in PSI core antenna. Chem Phys Lett 201: 535–542

Fairclough WV, Evans MCW, Purton S, Jones S, Rigby SEJ and Heathcote P (2001) Site-directed mutagenesis of PsaA: M684 in *Chlamydomonas reinhardtii*. In: PS2001 Proceedings: 12th International Congress on Photosynthesis. CSIRO Publishers, Melbourne, Australia

Frese RN, Palacios MA, Azzizi A, van Stokkum IHM, Kruip J, Rögner M, Karapetyan NV, Schlodder E, van Grondelle R and Dekker JP (2002) Electric field effects on red chlorophylls, β-carotenes and P700 in cyanobacterial Photosystem I complexes. Biochim Biophys Acta 1554: 180–191

Gatzen G, Müller MG, Griebenow K and Holzwarth AR (1996) Primary processes and structure of the photosystem II reaction center. 3. Kinetic analysis of picosecond energy transfer and charge separation processes in the D1-D2-cyt-b_{559} complex measured by time resolved fluorescence. J Phys Chem 100: 7269–7278

Germano M, Yakushevska AE, Keegstra W, van Gorkom HJ, Dekker JP and Boekema EJ (2002) Supramolecular organization of photosystem I and light-harvesting complex I in *Chlamydomonas reinhardtii*. FEBS Lett 525: 121–125

Gibasiewicz K, Ramesh VM, Lin S, Woodbury NW and Webber AN (2002) Excitation dynamics in eukaryotic PS I from *Chlamydomonas reinhardtii* CC 2696 at 10 K. Direct detection of the reaction center exciton states. J Phys Chem B 106: 6322–6330

Gobets B and van Grondelle R (2001) Energy transfer and trapping in photosystem I. Biochim Biophys Acta 1507: 80–99

Gobets B, van Amerongen H, Monshouwer R, Kruip J, Rögner M, van Grondelle R and Dekker JP (1994) Polarized site-selected fluorescence spectroscopy of isolated photosystem I particles. Biochim Biophys Acta 1188: 75–85

Gobets B, Dekker JP and van Grondelle R (1998a) Transfer-to-the-trap limited model of energy transfer in photosystem I. In: Garab G (ed) Photosynthesis: Mechanisms and Effects, pp 503–508. Kluwer Academic Publishers, Dordrecht, The Netherlands

Gobets B, van Stokkum IHM, van Mourik F, Rögner M, Kruip J, Dekker JP and van Grondelle R (1998b) Time-resolved fluorescence measurements of photosystem I from *Synechocystis*

PCC 6803. In: Garab G (ed) Photosynthesis: Mechanisms and Effects, pp 571–574. Kluwer Academic Publishers, Dordrecht, The Netherlands

Gobets B, van Stokkum IHM, Rögner M, Kruip J, Schlodder E, Karapetyan NV, Dekker JP and van Grondelle R (2001) Time-resolved fluorescence emission measurements of photosystem I particles of various cyanobacteria: a unified compartmental model. Biophys J 81: 407–424

Golbeck J, Xu W, Zybailov B, van der Est A, Pushkar J, Zech S, Stehlik D and Chitnis PR (2001) Electron transfer through the quinone acceptor in cyanobacterial Photosystem I. In: PS2001 Proceedings: 12th International Congress on Photosynthesis. CSIRO Publishing, Melbourne, Australia

Guergova-Kuras M, Boudreaux B, Joliot A, Joliot P and Redding K (2001) Evidence for two active branches for electron transfer in photosystem I. Proc Natl Acad Sci USA 98: 4437–4442

Hastings G, Kleinherenbrink FAM, Lin S and Blankenship RE (1994a) Time-resolved fluorescence and absorption spectroscopy of photosystem I. Biochemistry 33: 3185–3192

Hastings G, Kleinherenbrink FAM, Lin S, McHugh TJ and Blankenship RE (1994b) Observation of the reduction and reoxidation of the primary electron acceptor in photosystem I. Biochemistry 33: 3193–3200

Hastings G, Hoshina S, Webber AN and Blankenship RE (1995a) Universality of energy and electron transfer processes in photosystem I. Biochemistry 34: 15512–15522

Hastings G, Reed LJ, Lin S and Blankenship RE (1995b) Excited state dynamics in photosystem I: effects of detergent and excitation wavelength. Biophys J 69: 2044–2055

Hayes JM, Matsuzaki S, Rätsep M and Small GJ (2000) Red chlorophyll *a* antenna states of photosystem I of the cyanobacterium *Synechocystis* sp. PCC 6803. J Phys Chem B 104: 5625–5633

Hecks B, Wulf K, Breton J, Leibl W and Trissl H-W (1994) Primary charge separation in photosystem I – a two step electrogenic charge separation connected with $P_{700}^{+}\,A_{0}^{-}$ and $P700^{+}A_{1}^{-}$ formation. Biochemistry 33: 8619–8624

Hiyama T and Ke B (1971) A further study of P430: a possible primary electron acceptor of Photosystem I. Arch Biochem Biophys 147: 99–108

Holzwarth AR, Haehnel W, Ratajczak R, Bittersmann E and Schatz G (1990) Energy transfer kinetics in photosystem I particles isolated from *Synechococcus* sp. and from higher plants. In: Baltscheffsky M (ed) Current Research in Photosynthesis, pp 611–614. Kluwer Academic Publishers, Dordrecht, The Netherlands

Holzwarth AR, Schatz G, Brock H and Bittersmann E (1993) Energy transfer and charge separation kinetics in photosystem I Part I: picosecond transient absorption and fluorescence study of cyanobacterial photosystem I particles. Biophys J 64: 1813–1826

Holzwarth AR, Dorra D, Müller MG and Karapetyan NV (1998) Structure–function relationships and excitation dynamics in photosystem I. In: Garab G (ed) Photosynthesis: Mechanism and Effects, pp 497–502. Kluwer Academic Publishers, Dordrecht, The Netherlands

Ikegami I (1976) Fluorescence changes related to the primary photochemical reaction in the P700 enriched particles isolated from spinach chloroplasts. Biochim Biophys Acta 449: 245–258

Jennings RC, Zucchelli G, Croce R, Valkunas L, Finzi L and Garlaschi FM (1997) Model studies on the excited state equilibrium perturbation due to reaction centre trapping in photosystem I. Photosynth Res 52: 245–253

Joliot P and Joliot A (1999) *In vivo* analysis of the electron transfer within photosystem I: are the two phylloquinones involved? Biochemistry 38: 11130–11136

Jordan P, Fromme P, Witt HT, Klukas O, Saenger W and Krauß N (2001) Three-dimensional structure of cyanobacterial photosystem I at 2.5 Å resolution. Nature 411: 909–917

Karapetyan NV, Dorra D, Schweitzer G, Bezsmertnaya IN and Holzwarth AR (1997) Fluorescence spectroscopy of the long-wave chlorophylls in trimeric and monomeric photosystem I complexes from the cyanobacterium *Spirulina platensis*. Biochemistry 36: 13830–13837

Karapetyan NV, Holzwarth AR and Rögner M (1999) The photosystem I trimer of cyanobacteria: molecular organization, excitation dynamics and physiological significance. FEBS Lett 460: 395–400

Kargul J, Nield J and Barber J (2003) Three-dimensional reconstruction of a light-harvesting complex I- photosystem I (LHCI–PSI) supercomplex from the green alga *Chlamydomonas reinhardtii*. Insights into light harvesting for PSI. J Biol Chem 278: 16135–16141

Kennis JTM, Gobets B, van Stokkum IHM, Dekker JP, van Grondelle R and Fleming GR (2001) Light harvesting by chlorophylls and carotenoids in the photosystem I core complex of *Synechococcus elongatus*: a fluorescence upconversion study. J Phys Chem B 105: 4485–4494

Klug DR, Giorgi LB, Crystal B, Barber J and Porter G (1989) Energy transfer to low energy chlorophyll species prior to trapping by P700 and subsequent electron transfer. Photosynth Res 22: 277–284

Klukas O, Schubert W-D, Jordan P, Krauß N, Fromme P, Witt HT and Saenger W (1999) Photosystem I, an improved model of the stromal subunits PsaC, PsaD, and PsaE. J Biol Chem 274: 7351–7360

Krauß N, Hinrichs W, Witt. I, Fromme P, Pritzkow W, Dauter Z, Betzel C, Wilson KS, Witt HT and Saenger W (1993) Three-dimensional structure of system I of photosynthesis at 6 Å resolution. Nature 361: 326–331

Krauß N, Schubert WD, Klukas O, Fromme P, Witt HT and Saenger W (1996) Photosystem I at 4 Å resolution represents the first structural model of a joint photosynthetic reaction centre and core antenna system. Nat Struct Biol 3: 965–73

Kumazaki S, Iwaki M, Ikegami I, Kandori H, Yoshihara K and Itoh S (1994a) Rates of primary electron transfer reactions in the photosystem I reaction center reconstituted with different quinones as the secondary acceptor. J Phys Chem 98: 11220–11225

Kumazaki S, Kandori H, Petek H, Yoshihara I and Ikegami I (1994b) Primary photochemical processes in P700-enriched photosystem I particles – trap-limited excitation decay and primary charge separation. J Phys Chem 98: 10335–10342

Kumazaki S, Furusawa H, Yoshihara I and Ikegami I (1998) Excitation wavelength dependence of the excitation transfer in photosystem I reaction center with reduced number of antenna chlorophylls. In: Garab G (ed) Photosynthesis: Mechanisms and Effects, pp 575–578. Kluwer Academic Publishers, Dordrecht, The Netherlands

Kumazaki S, Ikegami I, Furusawa H, Yasuda S and Yoshihara K (2001) Observation of the excited state of the primary electron donor chlorophyll (P700) and the ultrafast charge separation

in the spinach photosystem I reaction center. J Phys Chem B 105: 1093–1099

Laible PD, Zipfel W and Owens TG (1994) Excited state dynamics in chlorophyll-based antennae: the role of transfer equilibrium. Biophys J 66: 844–860

Lüneberg J, Fromme P, Jekow P and Schlodder E (1994) Spectroscopic characterization of PS I core complexes from thermophilic *Synechococcus* sp.: identical reoxidation kinetics of A_1^- before and after removal of the iron–sulfur-clusters F_A and F_B. FEBS Lett 338: 197–202

Melkozernov AN (2001) Excitation energy transfer in photosystem I from oxygenic organisms. Photosynth Res 70: 129–153

Melkozernov AN, Su H, Lin S, Bingham S, Webber AN and Blankenship RE (1997) Specific mutations near the primary donor in photosystem I from *Chlamydomonas reinhardtii* alters trapping time and spectroscopic properties of P700. Biochemistry 36: 2898–2907

Melkozernov AN, Lin S and Blankenship RE (1998a) Energy equilibration in the antenna of photosystem I from cyanobacterium *Synechocystis* sp. PCC 6803. In: Garab G (ed) Photosynthesis: Mechanisms and Effects, pp 405–408. Kluwer Publishers, Dordrecht, The Netherlands

Melkozernov AN, Su H, Webber AN and Blankenship RE (1998b) Excitation energy transfer in thylakoid membranes from *Chlamydomonas reinhardtii* lacking chlorophyll *b* and with mutant photosystem I. Photosynth Res 56: 197–207

Melkozernov AN, Lin S and Blankenship RE (2000) Excitation dynamics and heterogeneity of energy equilibration in the core antenna of Photosystem I from the cyanobacterium *Synechocystis* sp. PCC 6803. Biochemistry 39: 1489–1498

Melkozernov AN, Kargul J, Lin S, Barber J and Blankenship RE (2004) Energy coupling in the PSI–LHCI supercomplex from the green alga *Chlamydomonas reinhardtii*. J Phys Chem. 108: 10547–10555

Mi D, Lin S and Blankenship RE (1999) Picosecond transient absorption spectroscopy in the blue spectral region of photosystem I. Biochemistry 38: 15231–15237

Muhiuddin IP, Heathcote P, Carter S, Purton S, Rigby SEJ and Evans MCW (2001) Evidence from time resolved studies of the $P700^+/A_1^-$ radical pair for photosynthetic electron transfer on both the PsaA and PsaB branches of the Photosystem I reaction centre. FEBS Lett 503: 56–60

Müller MG, Niklas J, Lubitz W and Holzwarth AR (2003) Ultrafast transient absorption studies on photosystem I reaction centers from *Chlamydomonas reinhardtii*. 1. A new interpretation of the energy trapping and early electron transfer steps in photosystem I. Biophys J 85: 3899–3922

Nuijs AM, Shuvalov VA, van Gorkom HJ, Plijter JJ and Duysens LNM (1986) Picosecond absorbance difference spectroscopy on the primary reactions and the antenna-excited states in photosystem I particles. Biochim Biophys Acta 850: 310–318

Owens TG, Webb SP, Alberte RS, Mets L and Fleming GR (1988) Antenna structure and excitation dynamics in photosystem I. I. Studies of detergent-isolated photosystem I preparations using time-resolved fluorescence analysis. Biophys J 53: 733–745

Pålsson L-O, Tjus SE, Andersson B and Gillbro T (1995) Energy transfer in photosystem I. Time resolved fluorescence of the native photosystem I complex and its core complex. Chem Phys 194: 291–302

Pålsson L-O, Dekker JP, Schlodder E, Monshouwer R and van Grondelle R (1996) Polarized site-selective fluorescence spectroscopy of long-wavelength emitting chlorophylls in isolated photosystem I particles of *Synechococcus elongatus*. Photosynth Res 48: 239–246

Pålsson L-O, Flemming C, Gobets B, van Grondelle R, Dekker JP and Schlodder E (1998) Energy transfer and charge separation in photosystem I: P700 oxidation upon selective excitation of the long-wavelength antenna chlorophylls of *Synechococcus elongatus*. Biophys J 74: 2611–2622

Ramesh VM, Gibasiewicz K, Lin S, Bingham SE and Webber AN (2004) Bidirectional electron transfer in photosystem I: accumulation of A_0 in A-side and B-side mutants of the axial ligand to chlorophyll A_0. Biochemistry 43: 1369–1375

Rätsep M, Johnson TW, Chitnis PR and Small GJ (2000) The red-absorbing chlorophyll *a* antenna states of photosystem I: a hole-burning study of *Synechocystis* sp. PCC 6803 and its mutants. J Phys Chem B 104: 836–847

Savikhin S, Wells T, Song P-S and Struve WS (1993) Ultrafast pump–probe spectroscopy of native etiolated phytochrome. Biochemistry 32: 7512–7518

Savikhin S, Buck DR and Struve WS (1999a) The Fenna-Matthews-Olson protein: a strongly coupled photosynthetic antenna. In: Andrews DL and Demidov AA (eds) Resonance Energy Transfer, pp 399–434. John Wiley & Sons, New York

Savikhin S, Xu W, Soukoulis V, Chitnis PR and Struve WS (1999b) Ultrafast primary processes in photosystem I of the cyanobacterium *Synechocystis* sp. PCC 6803. Biophys J 76: 3278–3288

Savikhin S, Xu W, Chitnis PR and Struve WS (2000) Ultrafast primary processes in PS I from *Synechocystis* sp. PCC 6803: roles of P700 and A_0. Biophys J 79: 1573–1586.

Savikhin S, Xu W, Martinsson P, Chitnis PR and Struve WS (2001) Kinetics of charge separation and $A_0^- - > A_1$ electron transfer in photosystem I reaction centers. Biochemistry 40: 9282–9290

Shubin VV, Murthy SDS, Karapetyan NV and Mohanty P (1991) Origin of the 77 K variable fluorescence at 758 nm in the cyanobacterium *Spirulina platensis*. Biochim Biophys Acta 1060: 28–36

Shuvalov VA, Nuijs AM, van Gorkom HJ, Smit HWJ and Duysens LNM (1986) Picosecond absorbance changes upon selective excitation of the primary electron donor P700 in photosystem I. Biochim Biophys Acta 850: 319–323

Struve WS (1995) Theory of electronic energy transfer. In: Blankenship RE, Madigan MT and Bauer CE (eds) Anoxygenic Photosynthetic Bacteria, pp 297–313. Kluwer Academic Publishers, Dordrecht, The Netherlands

Telfer A, Barber J, Heathcote P and Evans MCW (1978) Variable chlorophyll *a* fluorescence from P700 enriched photosystem I particles dependent on the redox state of the reaction centre. Biochim Biophys Acta 504: 153–164

Trinkunas G and Holzwarth AR (1996) Kinetic modeling of exciton migration in photosynthetic systems. 3. Application of genetic algorithms to simulations of excitation dynamics in three dimensional photosystem core reaction center complexes. Biophys J 71: 351–364

Trissl H-W (1997) Determination of the quenching efficiency of the oxidized primary donor of photosystem I, $P700^+$: implications for the trapping mechanism. Photosynth Res 54: 237–240

Turconi S, Schweitzer G and Holzwarth AR (1993) Temperature-dependence of picosecond fluorescence kinetics of a cyanobacterial photosystem-I particle. Photochem Photobiol 57: 113–119

Turconi S, Kruip J, Schweitzer G, Rönger M and Holzwarth AR (1996) A comparative fluorescence kinetics study of photosystem I monomers and trimers from *Synechocystis* PCC 6803. Photosynth Res 49: 263–268

Valkunas L, Liuolia V, Dekker JP and van Grondelle R (1995a) Description of energy migration and trapping in photosystem I by a model with 2 distance scaling parameters. Photosynth Res 43: 149–154

Valkunas L, Trinkunas G, Liuolia V and van Grondelle R (1995b) Nonlinear annihilation of excitations in photosynthetic systems. Biophys J 69: 1117–1129

van der Lee J, Bald D, Kwa SLS, van Grondelle R, Rönger M and Dekker JP (1993) Steady-state polarized-light spectroscopy of isolated photosystem-I complexes. Photosynth Res 35: 311–321

van Grondelle R (1985) Excitation energy transfer, trapping and annihilation in photosynthetic systems. Biochim Biophys Acta 811: 147–195

van Grondelle RJ, Dekker JP, Gillbro T and Sundstrom V (1994) Energy trapping and transfer in photosynthesis. Biochim Biophys Acta 1187: 1–65

Wasielewski MR, Fenton JM and Govindjee (1987) The rate of formation of $P700^{+} - A_0^{-}$ in photosystem I particles from spinach as measured by picosecond transient absorption spectroscopy. Photosynth Res 12: 181–190

Webber AN, Su H, Bingham SE, Käss H, Krabben L, Kuhn M, Jordan R, Schlodder E and Lubitz W (1996) Site-directed mutations affecting the spectroscopic characteristics and midpoint potential of the primary donor in photosystem I. Biochemistry 35: 12857–12863

Werst M, Jia Y, Mets L and Fleming GR (1992) Energy transfer and trapping in the photosystem I core antenna. A temperature study. Biophys J 61: 868–878

White NTH, Beddard GS, Thorne JRG, Feehan TM, Keyes TE and Heathcote P (1996) Primary charge separation and energy transfer in the photosystem I reaction center of higher plants. J Phys Chem 100: 12086–12099

Wittmershaus BP, Woolf VM and Vermaas WFJ (1992) Temperature dependence and polarization of fluorescence from photosystem I in the cyanobacterium *Synechocystis* sp PCC 6803. Photosynth Res 31: 75–87

Woodbury NW and Allen JP (1995) The pathway, kinetics and thermodynamics of electron transfer in wild type and mutant reaction centers of purple nonsulfur bacteria. In: Blankenship RE, Madigan MT and Bauer CE (eds) Anoxygenic Photosynthetic Bacteria. Kluwer Academic Publishers, Dordrecht, The Netherlands

Xu W, Chitnis PR, Valieva A, van der Est A, Brettel K, Guergova-Kuras M, Pushkar YN, Zech SG, Stehlik D, Shen G, Zybailov B and Golbeck JH (2003a) Electron transfer in cyanobacterial photosystem I: II. Determination of forward electron transfer rates of site-directed mutants in a putative electron transfer pathway from A_0 through A_1 to F_X. J Biol Chem 278: 27876–27887

Xu W, Chitnis PR, Valieva A, van der Est A, Pushkar YN, Krzystyniak M, Teutloff C, Zech SG, Bittl R, Stehlik D, Zybailov B, Shen G and Golbeck JH (2003b) Electron transfer in cyanobacterial photosystem I: I. Physiological and spectroscopic characterization of site-directed mutants in a putative electron transfer pathway from A_0 through A_1 to F_X. J Biol Chem 278: 27864–27875

Zazubovich V, Matsuzaki S, Johnson TW, Hayes JM, Chitnis PR and Small GJ (2002) Red antenna states of photosystem I from cyanobacterium *Synechococcus elongatus*: a spectral hole burning study. Chem Phys 275: 47–59

Author: Please provide forename for "Govindjee" in Wasielewski et al. (1987).